A remote sensing image self-adaptive blind watermarking algorithm based on wavelet transformation

XUN WANG, YI OU-YANG, AND HUA-MAO GU
College of Computer & Information Engineering
Zhejiang Gongshong University
Jiao Gong Road No. 149, Hangzhou, Zhejiang
CHINA

Abstract: -Based on the statistical characters of remote sensing image, this paper proposed firstly partition remote sensing image into sub-block images of suitable sizes, and then decomposing these sub-block images with biorthogonal 7/5 wavelet. A novel construction method of wavelet set of coefficients is adopted to embed binary watermarking image into sub-bands except low frequency sub-bands, and realizing a blind detection algorithm. The visual model of biorthogonal 9/7 wavelet is extended to construct a visual weighted analysis method based on the biorthogonal 7/5 wavelet domain quantization noises, thus making the strength of the embedded watermarking could self-adapt to the sub-blocks of the remote sensing image. Experimental results show that the proposed algorithm has great imperceptibility and is robust to the image intensity attack such as geometric transformation, noise adding, filtering, and compression. It performs better than that of the watermarking algorithm proposed by Ho in the robust, and being a practical blind watermarking algorithm.

Key-Words: - blind watermarking; wavelet tranformation; remote sensing image

1 Introduction

Remote sensing images contain huge amounts of information, even confidential information, so these tremendously precious image data have great economic and military value. But the research has just initiated on intellectual property right protection of remote sensing image, referring to the related documents [1-5] and so on. Document [1] proposed embedding pseudo-random binary sequence watermarking into the middle frequency coefficient of the DFT transformation domain and three high frequency sub-bands of DWT. Since this embedding process conforms to the near-lossless constraint demands, so the robustness of the watermarking is enhanced. Document [2] proposed a non-sequential spread spectrum based remote sensing image watermarking algorithm, which utilizes the corresponding characters of non-sequential information to embed and extract watermarking. Compared with common spread spectrum watermarking algorithm, the robustness of this algorithm is sharply enhanced. Based on the characters of remote sensing image, document [3] proposed conducting Arnold permutation encryption and image compression on gray-level watermark image, and embedding the processed image into the wavelet transformation domain of remote sensing images, adopting the neighboring symbol's mean value method, odd-even adjudging rule method. Document [4] proposed a novel remote sensing image watermarking algorithm, which adopts the character of spatial masking to calculate the maximum limitation of the change of every DCT coefficient. Document [5] proposed securely embedding binary watermarking image into the high-frequency coefficients of the discrete cosine transformation domain of the remote sensing image texture. On the basis of the above-mentioned researches, this paper proposed a self-adaptive blind watermarking algorithm on remote sensing image, adopting the visual weighted analysis method of the visual system biorthogonal 7/5 wavelet domain quantization noises.

2 Related theories

2.1 Lifting algorithm of biorthogonal 7/5 wavelet filter

According to the document [6], suppose x_i is the inputting sequence of image data, and then the Lazy wavelet is defined as:

$$s_j^{(0)} = x_{2j}, \quad d_j^{(0)} = x_{2j+1}$$

The positive lifting algorithm for 7/5 wavelet is listed as:

$$\left.\begin{array}{ll} Step1 & s_j^{(1)} = s_j^{(0)} + \alpha(d_j^{(0)} + d_{j-1}^{(0)}) \\ Step2 & d_j^{(1)} = d_j^{(0)} + \beta(s_j^{(1)} + s_{j+1}^{(1)}) \\ Step3 & s_j^{(2)} = s_j^{(1)} + \gamma(d_j^{(1)} + d_{j-1}^{(1)}) \\ Step4 & s_j = Ks_j^{(2)} \\ Step5 & d_j = d_j^{(1)} / K \end{array}\right\} \quad (1)$$

Where,

$$\beta = -\frac{1}{4\alpha+2}, \quad \gamma = \frac{1-4\alpha^2}{4}, \quad K = \frac{1}{2\alpha+1} \quad (2)$$

From the experimental results of document [6], best performance of image compression could be achieved when α=0.05.

2.2 Preprocessing of watermark

The permutation technology of digital watermarking mainly considers dispersing error distribution as far as possible, improving the visual effects to enhance the robustness of digital watermarking. Of current available permutation methods, Arnold permutation is simple, easy to implement and with cycles. When the remote sensing image is modified by user or under malicious attacks, some parts of the remote sensing image will be damaged, so will be the corresponding watermarks. Since Arnold transformation maximally disperses the damaged bits into different parts of the watermarks, the effects on visual system will be reduced and the watermark robustness is improved.

For 2-D image, Arnold transformation formula is:

$$\begin{pmatrix} x' \\ y' \end{pmatrix} = \begin{pmatrix} 1 & 1 \\ 1 & 2 \end{pmatrix} \begin{pmatrix} x \\ y \end{pmatrix} \left(\mathrm{mod} \quad \tilde{N}\right) \quad (3)$$

In which, $x, y \in (0,1,2,\cdots,N-1)$, representing the coordinates of a pixel, while N is the image matrix divisor.

Normally, for different image matrix divisors N, Arnold permutation will have different transformation cycles, but the calculation of image restoration based on the cycle is quite huge. This paper proposes adopting equation solving to obtain Arnold anti-transformation algorithm. The obtained Arnold anti-transformation formula is [7]:

$$\begin{pmatrix} x \\ y \end{pmatrix} = \begin{pmatrix} 2 & -1 \\ -1 & 1 \end{pmatrix} \begin{pmatrix} x' \\ y' \end{pmatrix} \mathrm{mod}\, \tilde{N}. \quad (4)$$

3 Principle of watermark embedding

3.1 HVS based remote sensing image segmentation

Watermark embedding process could be regarded as superposing a weak signal to a strong background, thus HVS could not detect the existence of a signal if it is below the HVS contrast sensitivity threshold. Based on HVS and the statistic characters of remote sensing image, remote sensing image is segmented to many sub-blocks of same size. Different amplitude quantization could be performed on the basis of different regional characters of sub-blocks. The detailed method is described as follows:

Suppose the remote sensing image is I, in accordance with the size of I, the image will be self-adaptively partitioned into sub-blocks with the size of 512×512 bits, denoted as $I_K = f_k(x,y)$, $k = 0,1,\cdots,k-1$. Entropy value and variance are calculated for every sub-block, in which the image block with a small entropy value relates to smooth areas, while the sub-block with a large entropy value relates to textures or edges. Furthermore, the variance for textures is small, and the variance for edges is large. So all the image blocks could be categorized into four types, and an amplitude quantization will be assigned to each type.

For type 1, with low illumination and simple texture, HVS is quite sensitive to the change of the pixel, so the smallest amplitude quantization should be assigned. For type 2, with relatively high illumination, complex textures being edges, the amplitude quantization should be relatively small. For type 4, with high illumination, complex textures but not being edges, HVS is least sensitive to the change of the pixel, so the largest amplitude quantization should be assigned. The remaining sub-blocks could be partitioned into type 3. Specific amplitude quantization could be obtained through experiment. Based on the documents [1, 9] and experimental analysis, this paper considers following amplitude quantization as reasonable values: 8 is assigned for type 1, 10 is assigned for type 2, 16 is assigned for type 3 and 32 is assigned for type 4.

3.2 Wavelet domain quantization noises based visual weighted analysis

For 512×512 bits sub-blocks, by means of multi-resolution wavelet decomposition, the image could be decomposed into sub-band LL and detailed sub-bands $LHi, HLi, HHi \quad (i = 1,2,\cdots,k)$ corresponding to the horizontal, vertical and diagonal directions, in which k is the decomposition layer.

The decomposition process of multi-resolution wavelet transformation has fairly excellent spatial direction, which coincides with human visual characters, so Just Noticeable Distortion (JND) tolerance based on human visual characteristics could be precisely established. With JND tolerance, watermark embedding position and strength will be controlled to ensure the visual imperceptibility of the

watermark. Documents [10-12] have set up different models for wavelet domain JND tolerance.

Document [11] studied the quantization noises in image compression adopted biorthogonal 9/7 wavelets, and provided visual models for different sub-bands, targeting at the images with gray-level values between 0 and 255.

$$Q_{l,f} = \frac{2}{A_{l,f}} \alpha 10^{l\left(\log \frac{2^l f_o g_f}{r}\right)^2}$$

According to the Watson visual model, l represents the multi-resolution decomposition layer, with possible values of 1, 2, 3 or 4. In the model, f represents the frequency direction, with values 1, 2, and 3 denoting the detailed sub-bands of horizontal, vertical and diagonal directions respectively, $A_{l,f}$ is the basis functions of sub-bands, r represents the visual resolution, α is the minimum value of the domain. The function with α＝0.495 is defined as:

$$g_f = \begin{cases} 1, & f = 1 \\ 1, & f = 2 \\ 0.534, & f = 3 \end{cases}$$

Thus, the quantization factors for wavelet coefficients of different layers without causing image distortion are listed in Table1.

Table 1 The quantization factors of biorthogonal 9/7 wavelet 3-layer transformation

l	f=1	f=2	f=3
1	23.03	23.03	58.76
2	14.68	14.69	28.41
3	12.71	12.71	19.54

Since the image quantization matrix is put forward on the basis of HVS, the matrix has provided the maximum noise-tolerant capability for different decomposition scales. Biorthogonal wavelet transformation is adopted to realize digital watermarking algorithm for remote sensing image. Complying with the prerequisite of watermark imperceptibility, the watermark is linked to the embedding strength to obtain JND with value $T_{l,f}=[\beta Q_{l,f}/2]$, where [·] represents rounding-off and β is the scale factor.

For biorthogonal 9/7 wavelet filters $\{h, g, \tilde{h}, \tilde{g}\}$, when the coefficients take values as $h_3 = 0,\ t = 1$, the biorthogonal 9/7 wavelet filter is actually a biorthogonal 7/5 wavelet filter. So, this paper roughly regards that for biorthogonal 7/5 wavelet filter, the quantization factors of various layers of wavelet coefficients could also take the values of Table 1.

3.3 Watermark embedding algorithm

For remote sensing image, it should be segmented into 512×512 sub-blocks first and then categorized into different types. According to these sub-blocks of different types, the quantization factors of 3-layer transformation will be adjusted. As this paper simply takes the processes linearly, the remote sensing images of type 3 are considered as base points and the quantization difference of different types will be superposed to obtain quantization factors shown Table 2.

Table 2 The quantization factors of biorthogonal 7/5 wavelet 3-layer transformation for different types of image

Image types	l	f=1	f=2	f=3
Type 1	1	15.03	15.03	50.76
	2	6.68	6.68	20.41
	3	4.71	4.71	11.54
Type 2	1	17.03	17.03	52.76
	2	8.68	8.68	22.41
	3	6.71	6.71	13.54
Type 3	1	23.03	23.03	58.76
	2	14.68	14.68	28.41
	3	12.71	12.71	19.54
Type 4	1	39.03	39.03	74.76
	2	30.68	30.68	44.41
	3	28.71	28.71	35.54

For remote sensing image with the size of 512×512 bits, the detailed embedded procedures are described as below.

Biorthogonal 7/5 wavelet 3-layer decomposition is conducted on the remote sensing image with the size of 512×512 bits. All the coefficients after decomposition are selected to make up the coefficient sequence except LL3 coefficients. The following procedures are taken to generate the set of coefficients $\{M_o\}$ for watermark embedding. o represents the number of times of watermark embedding, with possible values as $o = 2,3,4,5,\cdots$ for different circumstances.

(1) Searching for the maximum absolute value of wavelet coefficient $W_{\max}$;

(2) Calculating T, $T = 2^{[\log_2 W_{\max}]}$, then $T < W_{\max} < 2T$;

(3) Given a threshold G, calculating the maximum possible embedding times S, where $\left|T / 2^s\right| > G$;

(4) According to the watermark image with size I (for example, the watermark embedding image is 64×64, then I=64×64=4096), a set of coefficients for embedding is generated:

a) $M_0 = \{w_l^f(i,j,0), w_l^f(i,j,1), \cdots, w_l^f(i,j,r_0)\}$,

satisfying: $|w_l^f(i,j,k)| \in [\frac{n_0 \cdot T}{2^m},\ 2T),\ r_0 \geq I-1$,

where $n_0 = 1,2,\cdots,2^S$.

b) $M_1 = \{w_l^f(i,j,0), w_l^f(i,j,1), \cdots, w_l^f(i,j,r_1)\}$,

satisfying: $|w_l^f(i,j,k)| \in [\frac{n_1}{2^S} \cdot T,\ \frac{n_0}{2^S} \cdot T),\ r_1 \geq I-1$,

where $n_1 = 1,2,\cdots,2^S$.

c) $M_{\max} = \{w_l^f(i,j,0), w_l^f(i,j,1), \cdots, w_l^f(i,j,r_{mzx})\}$, satisfying:

$$|w_l^f(i,j,k)| \in [\frac{n_{mzx}}{2^S} \cdot T,\ \frac{n_{mzx-1}}{2^S} \cdot T),\ r_{mzx} \geq I-1$$,

where $n_{\max} = 1,2,\cdots,2^S$.

Where l and f have the same meanings as described in the above section, representing the wavelet decomposition layer and sub-band directions respectively, i and j individually represent the horizontal and vertical coordinates of the wavelet coefficient matrix, and r_k represents a value within a certain domain which is larger than the watermark image size I.

From the process of coefficient set generating, under the circumstances that the remote sensing image is of 512×512 bits and the binary embedding image is of 64×64bits, at least one coefficient set for embedding could be obtained. Generally, through adjusting the threshold G, the number of the set of coefficients for embedding is greater than three.

(5) All sets of coefficients for embedding M_i are modified, and watermarks are embedded repetitively:

a) When the value of watermark signal equals one, $\tilde{w}_l^f(i,j,k) = \lfloor w_l^f(i,j,k)/T_{l,f} \rfloor \times T_{l,f} + \alpha \times \frac{T_{l,f}}{2}$;

b) When the value of watermark signal equals zero, $\tilde{w}_l^f(i,j,k) = \lfloor w_l^f(i,j,k)/T_{l,f} \rfloor \times T_{l,f} - \alpha \times \frac{T_{l,f}}{2}$;

Where $T_{l,f}$ is the amplitude modification for JND, α is the scale factor with $\alpha \in (0,\ 1)$, and $\lfloor \bullet \rfloor$ represents the integer floor function.

3.4 Watermark extracting algorithm

Watermark extracting procedure is just the inverse of embedding one, and details are described as below:

(1) Biorthogonal 7/5 wavelet 3-layer decomposition is conducted on the remote sensing image with the size of 512×512 bits. All the coefficients after decomposition are selected to make up the coefficient sequence except LL3 coefficients. The following procedures are taken to generate the set of coefficients $\{M_o\}$;

(2) Searching for the maximum absolute value of wavelet coefficient $\tilde{W}_{\max}$;

(3) Calculating $\tilde{T}, \tilde{T} = 2^{\lceil \log_2 \tilde{W}_{\max} \rceil}$, then $\tilde{T} < \tilde{W}_{\max} < 2\tilde{T}$;

(4) With the embedded value S, the set of coefficients for embedding could be obtained:

a) $\tilde{M}_0 = \{\tilde{w}_l^f(i,j,0), \tilde{w}_l^f(i,j,1), \cdots, \tilde{w}_l^f(i,j,\tilde{r}_0)\}$,

satisfying: $|\tilde{w}_l^f(i,j,k)| \in [\frac{n_0 \cdot \tilde{T}}{2^S},\ 2\tilde{T})$.

b) $\tilde{M}_1 = \{\tilde{w}_l^f(i,j,0), \tilde{w}_l^f(i,j,1), \cdots, \tilde{w}_l^f(i,j,\tilde{r}_1)\}$,

satisfying: $|\tilde{w}_l^f(i,j,k)| \in [\frac{n_1}{2^S} \cdot \tilde{T},\ \frac{n_0}{2^S} \cdot \tilde{T})$.

c) $\tilde{M}_{\max} = \{\tilde{w}_l^f(i,j,0), \tilde{w}_l^f(i,j,1), \cdots, \tilde{w}_l^f(i,j,\tilde{r}_{mzx})\}$,

satisfying: $|\tilde{w}_l^f(i,j,k)| \in [\frac{n_{mzx}}{2^S} \cdot \tilde{T},\ \frac{n_{mzx-1}}{2^S} \cdot \tilde{T})$.

Where the values of n_i and S is identical to those of the embedding procedure.

(5) With the value of $\tilde{W}_l^f(i,j,k)$, the corresponding embedding watermark signal I_k^o will be obtained, either one or zero;

(6) Various sets of coefficients are integrated to obtain I_k^o and the watermark sequence I_k ;

(7) Sorting I_k to get the watermark sequence I', and T/2 times of Arnold permutations are conducted on I' to obtain the watermark sequence Q' .

∗ Note: The extracting procedure of step 5 is explained as below:

Formula $\lfloor w_l^f(i,j,k)/T_{l,f} \rfloor \times T_{l,f}$ is actually an $N \times T_{l,f}\ (where, N = 0,1,2\cdots)$ integer round function. Namely, if $w_l^f(i,j,k) \in [0, T_{l,f})$, then $\lfloor w_l^f(i,j,k)/T_{l,f} \rfloor \times T_{l,f} = 0$, and if $w_l^f(i,j,k) \in [T_{l,f}, 2T_{l,f})$, then $\lfloor w_l^f(i,j,k)/T_{l,f} \rfloor \times T_{l,f} = T_{l,f}$, and so on. When $0 < \alpha \leq 1$, with the range of $\tilde{w}_l^f(i,j,k)$, the value of watermark signal could be determined, either one or zero:

$$I_k^o = \begin{cases} 1 & \tilde{w}_l^f(i,j,k) \in [N \cdot T_{l,f}, \frac{2N+1}{2} \cdot T_{l,f}) \\ 0 & \tilde{w}_l^f(i,j,k) \in [\frac{N-1}{2} \cdot T_{l,f}, N \cdot T_{l,f}) \end{cases}$$,

$where, N = 0,1,2\cdots$

4 Experimental results and discussion

The watermark used in the experiment is a 64×64 binary image (a) as shown in Figure 1. With Arnold permutation, images (b) and (c) in Figure 1 could be obtained, in which, image (b) is the watermark image after one permutation, while image (c) is the watermark after eight permutations and is actually embedded in the experiment.

(a) Original image (b) One permutation (c) Eight permutations

Fig.1 Watermark image

The experimental 512×512 remote sensing images are panchromatic images shown in Figure 2, in which image (a) is navigation image and image (b) is satellite one. The scale factors are set as β=0.1, $\alpha = 0.5$.

(a) (b)

Fig.2 Original remote sensing image

(a) (b)

Fig.3 Images after watermark embedding

Figure 3 is obtained after embedding watermark of figure 1 into the remote sensing images. The PSNR of the remote sensing images of embedded watermarking is calculated respectively, which is greater than 45db. From the visual perception, there is hardly any noticeable change, indicating the excellent imperceptibility of the algorithm. Watermark extracted is shown in Figure 4, as the images are almost identical to the original ones, with fine visual perception.

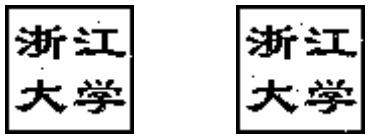

(a) (b)

Fig.4 Watermark extracted from Figure 3

To verify the effectiveness of the algorithm, a series of attacks was conducted on these remote sensing images after watermark embedded. JPEG compression with a quality factor of 60%, addition of zero mean Gaussian noises, two-times enlargement, and median filter are conducted respectively on these two remote sensing images of Figure 3. The results of watermark extracting are shown in Figures 5-8.

(c) (b)

Fig.5 JPEG compression with a quality factor of 60%

(e) (b)

Fig.6 Addition of zero mean Gaussian noises

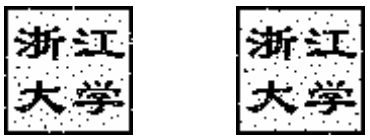

(g) (b)

Fig.7 Two-times enlargement

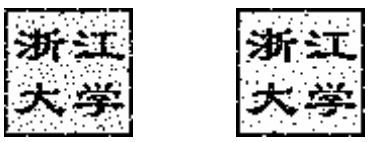

(i) (b)

Fig.8 Median filter (window size of 3×3)

It could be visually perceived that with two-times enlargement processing; there is no great influence

on the quality of the extracted watermark, namely excellent robustness. JPEG compression with a quality factor of 60%, addition of zero mean Gaussian noises, and median filter influenced the watermark images, but the watermark resolution is not affected and the quality of watermark is within the range of visual tolerance. For these four processing, addition of zero mean Gaussian noises had the greatest influence on watermark quality, but these two original images had no distinct influence on the quality of watermark extracted.

Furthermore, the algorithm proposed in this paper has been tested against various attacks, and was compared with Ho's algorithm [5]. Watermark images are extracted, and the accuracy rate is calculated with the following formula:

$$accuracy\_rate(\mathrm{P}) = \frac{total\_pixels - erroneous\_pixels}{total\_pixels} \times 100\%$$

According to algorithm proposed in this paper and document [4] respectively, the experimental results of figure 1 are shown in table 3. For attacking tests, the experimental results with the algorithm proposed is much better than that of Ho's algorithm, and the accuracy rates for watermark extracted from these two images exceeded 80%. The proposed wavelet domain based blind watermarking algorithm on remote sensing image is much robust against various geometric transformation, filtering and compression.

Table 3 Experimental results of watermark attacks

Attacks	Accuracy rate (P) %			
	Fig 1 (a)		Fig 1 (b)	
	Our Algorithms	Ho's Algorithms	Our Algorithms	Ho's Algorithms
Two-times enlargement	97.84	84.64	97.06	82.83
Two-times contraction	85.32	80.36	84.13	78.54
JPEG compress-ion (factors 60%)	94.38	74.49	93.75	69.26
JPEG compress-ion (factors 40%)	84.89	67.85	84.43	63.86
Rotation (3^0)	89.97	81.72	90.42	81.46
Rotation (5^0)	81.67	76.41	81.18	70.42
Addition of zero mean Gaussian noises	92.91	75.82	91.45	80.12
Median filter (3×3)	90.14	89.23	89.81	88.53
Median filter (5×5)	83.19	83.78	83.93	82.14
Addition of salt and-pepper noise	86.13	84.64	84.31	81.68

5 Conclusion

This paper proposed a self-adaptive blind watermarking algorithm based on the textures of remote sensing images and the statistical characters of the frequency after wavelet decomposition. This algorithm utilizes equation-solving method to realize Arnold permutation, so as to avoid the huge calculation costs in multiple permutations and anti-permutations. Biorthogonal 7/5 wavelet transformation with lifting parameter α=0.05 is adopted to extend the visual weighted analysis method based on the visual system (HVS) biorthogonal 7/5 wavelet domain quantization noises, so that the embedding strength could be self-adaptive to the sub-blocks of remote sensing images. A certain policy is adopted to embed binary watermark image into the sub-bands except low frequency sub-bands, and the extraction process is independent from the original image. Experimental results show that the proposed blind watermarking algorithm is robust and imperceptible, with the feature of high accuracy rate for watermark extracting. This algorithm is robust against geometric transformation, filtering and compression. It performs better than that of the watermarking algorithm proposed by Ho in the robust, and being a practical blind watermarking algorithm.

References:

[1] M. Barni, F. Bartolini, E. Magli et al. Watermarking techniques for electronic delivery of remote sensing images. *Optical Engineering*, 41(9), 2002, pp. 2111-2119.

[2] S. Chen, H. Leung, Chaotic spread spectrum watermarking for remote sensing images. *Journal of Electronic Imaging*, 13(1), 2004, pp. 220-230.

[3] XianMin Wang, ZeQun Guan, ChenHan Wu, The self-adaptive 2-dimension blind watermarking algorithm on remote sensing image, *Journal of computer engineering and applications*, 20, 2004, pp.37-41.

[4] Ho, et al. Robust Copyright Protection of Satellite Images Using a Novel Digital Image-in-image Watermarking Algorithm. *IEEE IGARSS' 01*. Sydney, 2001, pp. 1194-1196.

[5] XiangYang Wang, HongYin Yang, Jun Wu, Content-based discrete cosine transformation domain of self-adaptive digital watermarking algorithm on remote sensing image. *Acta Geodaetica et Cartographica Sinica*, 34(4), 2005, pp.324-330.

[6] M. Unser, T. Blu, Mathematical properties of the JPEG2000 wavelet filters. *IEEE Trans on Image Processing*, 12(9), 2003, PP: 1080-1090.

[7] Tao Kong, Dan Zhang. A new algorithm of Arnold anti-transformation. *Journal of Software*,15(10), 2004, pp: 1558-1564.

[8] WenJun Sun. Integer wavelet transformation based full-color compression technology on remote sensing image. *Doctor dissertation of Graduate University of the Chinese Academy of Sciences*. 2003.

[9] M. Barni, F. Bartolini, V. Cappellini et al. Copyright protection of remote sensing imagery by means of digital watermarking. *In: Proceedings of the SPIE-The International Society for Optical Engineering*, 2001, pp.4540: 565-576.

[10] A. S. Lewos, G. Knowles. Image compression using the 2-D wavelet transform. *IEEE trans. Image Proc*. 1(2), 1992, pp: 244-250.

[11] A. B. Watson, G. Y. Yang, Visibility of wavelet quantization noise. *IEEE Trans. On Iamge Processing*, 6(8), 1997, pp: 1164-1174.

[12] M. D. Swanson. Robust audio watermarking using perceptual marking. *Signal Processing*, 66(3), 1998, pp: 337-355.

Acknowledgment

This work is supported in part by the grand foundation of science and technology department of Zhejiang province under grant No. 2006C13098, the key foundation of education department of Zhejiang province under grant No. 20050642.